Proceedings of the 8th IEEE Mediterranean Conference
on Control and Automation (MED 2000)
Rio, Patras, GREECE 17-19 July, 2000

Decision Feedback Differentially Detected GMSK signals In the Presence of ACI and Nonlinearities

P. Takis Mathiopoulos
Department of Electr. and Comp. Engg.
University of British Columbia
Vancouver, BC, Canada

Jagdeep S. Toor
Wireless Local Techn. Group
AT&T
Seattle, USA

Abstract

The effects on the performance of differentially detected Gaussian Minimum Shift Keying (GMSK) signals operated in the presence of adjacent channel interference (ACI), modulator impairments, amplifier nonlinearities and additive white Gaussian noise (AWGN) is investigated. By means of computer simulation, the bit error rate (BER) performance of 1- and 2-bit conventional and decision feedback differentially detected (C-DD and DF-DD) GMSK systems in the presence of static and Rayleigh faded ACI is obtained. It is found that the best performance is achieved by the 2-bit DF-DD receiver and has resulted in BER performance improvements for the static ACI channel and error floor reductions for the Rayleigh faded ACI channel.

I. Introduction

The adoption of Gaussian Minimum Shift Keying (GMSK) signals [1], as the transmission standard for various wirelss mobile telecommunication systems, such as the pan-European digital cellular network (GSM) [2] and the digital European cordless telecommunications (DECT) [3], has established its importance as a modulation scheme.

Among the various signal detection techniques which can be employed in conjunction with GMSK signals, decision feedback differential detection (DF-DD) has been proposed to improve the performance of conventional differentially detected (C-DD) GMSK schemes [4], [5]. Although in the past, the DF-DD technique has been considered under different operating conditions, including the additive white Gaussian noise (AWGN) channel [4], fading [5], [6], and co-channel interference (CCI) [7], so far it has not been investigated in the presence of adjacent channel interference (ACI). Despite the fact that for cellular mobile radio systems, ACI is a less problematic interference as compared to CCI, it nevertheless still represents a non-negligible source of interference and thus system performance degradation [8], [10]. Furthermore, for non-cellular type of communication systems, especially for bandwidth and power efficient frequency division multiple access (FDMA) systems, ACI is one of the prominent sources of interference (see for example [9], [10], [11], [12]). Additionally, an intentional increase of ACI, for example by reducing the frequency channel spacing between adjacent channels, could significantly increase the overall spectral efficiency of the communication system under consideration [10], [13], [19].

Another type of discortion that usually is not considered in constant envelope schemes, such as an ideal GMSK signal[1], is nonlinear distortion. Such distortion is typically due to the presence of a nonlinear amplifier [14]. It is well accepted that for a constant envelope scheme, nonlinear amplification has little effects on the spectrum and the overall system performance [15]. However, hardware implementation imperfections, such as, for example, modulator deficiencies, would result in a non-constant envelope (i.e. nonideal) GMSK signal [16]. When such a nonideal, nonconstant envelope GMSK signal is passed through a nonlinear amplifier, it results in spectral spearding and thus creates additional ACI. Motivated by the above, in this paper we investigate the performance of DF-DD receivers in conjunction with ideal and nonideal GMSK signals in the presence of static and faded ACI and nonlinearities.

II. Communication System Model

Following [15], the transmitted GMSK signal can be mathematically represented as

$$s(t) = A_0 \cos[2\pi f_c t + \phi(t)] \tag{1}$$

where A_0 is a constant amplitude, f_c is the carrier frequency and $\phi(t)$ is given by

$$\phi(t) = \pi \sum_l b_l \int_{-\infty}^{t} g(\beta - lT)d\beta. \tag{2}$$

In the above equation, T is the bit duration, $g(t)$ is the impulse response of the well-known Gaussian low pass filter (GLPF), which has a normalized 3-dB bandwidth B_tT, and b_l=$-a_lb_{l-1}$, where a_l are independent and equiprobable information bits taking values from the alphabet $\{\pm 1\}$. As was pointed out in [4], for the 1-bit differential detector, differential encoding is not needed and thus for this case, b_l=a_l. Expanding Eq. (1), $s(t)$ can be expressed in

[1]The term "ideal GMSK signal" refers to an ideal, i.e. constant envelope, GMSK signal.

an equivalent in-phase (I-) and quadrature-phase (Q-) form as

$$s(t) = s_I(t)A_0\cos(2\pi f_c t) - s_Q(t)A_0\sin(2\pi f_c t) \quad (3)$$

where $s_I(t)$=cos[$\phi(t)$] and $s_Q(t)$=sin[$\phi(t)$]. Theoretically, an ideal Quadrature Modulator (QM) does not introduce any signal distortion. However, in practice nonideal components of the QM will introduce signal distortions, including signal imbalances and offsets between the I- and Q-channels. In [16], the effects of QM deficiencies on the transmitted signal have been identified as differential amplitude imbalance (Δ), local oscillator breakthrough and DC offsets (k), and differential phase error (θ_d) which can also be represented as differential time delay (τ_d), with $\tau_d = 2T\theta_d/\pi$. Mathematically, it is convenient to group all these QM deficiencies together in one of the channels, e.g. the I-channel. This is illustrated in Fig. 1. Therefore, for such a nonideal QM (NI-QM), the distorted GMSK signal $s'(t)$ can be mathematically expressed as

$$s'(t) = \sqrt{\{k + \Delta\cos[\phi(t-\tau_d)]\}^2 + \sin^2[\phi(t)]} \quad (4)$$
$$\times \cos[2\pi f_c t + \tan^{-1}\frac{\sin[\phi(t)]}{k + \Delta\cos[\phi(t-\tau_d)]}].$$

It is evident that $s'(t)$ is no longer a constant envelope scheme, exept for k=0, Δ=1 and τ_d=0. Clearly, in this specific case $s'(t)$=$s(t)$, which is an ideal GMSK signal. Following [16], we have considered the following two sets of values for modelling the imperfections of the NI-QM

1. $\theta_d = 1^o$, $\Delta = 0.95$, k = - 24 dB (refered to as "typical values"),
2. $\theta_d = 15^o$, $\Delta = 0.65$, k= - 12 dB (refered to as "extreme values").

As shown by the phase state-space diagrams of Fig. 2, the distortion which is introduced to the transmitted GMSK signal by the "extreme values" (Fig. 2b) is much more prominent as compared to the distortion caused by the "typical values" (Fig. 2a).

As illustrated in Fig. 3, the NI-QM could be followed by a nonlinear amplifier (NLA). We have considered two types of amplifier nonlinearities, namely the "mild nonlinearity" and the "severe nonlinearity". For the mild nonlinearity, we have used the fifth order Volterra series model given in [20]

$$s''(t) = s'(t)(G_1 + G_3 \mid s'(t) \mid^2 + G_5 \mid s'(t) \mid^4) \quad (5)$$

where $\mid \bullet \mid$ denotes absolute value. The complex coefficients G_1, G_3 and G_5 have been selected as G_1=1, G_3 = 0.0479$\angle$-2.816 rad and G_5 = 0.00102$\angle$0.39 rad. The AM-AM and AM-PM characteristics of this model were calculated and are plotted in Fig. 4, where the output signal amplitute and phase is plotted versus the input signal amplitude. Typically, the AM-AM and AM-PM characteristics of this model correspond to a class AB power amplifier [20].

For the severe nonlinearity, we have used the transfer function of a hard-limiter (HL), which is given by

$$s''(t) = s'(t)/\mid s'(t) \mid . \quad (6)$$

The HL has been used in the past by others to simulate the effects of an extremely highly nonlinear amplifier [19].

Assuming that the m-th adjacent channel interferer $i_m(t)$ is of the same modulation format as $s(t)$, it can be expressed as

$$i_m(t) = B_m\cos[2\pi(f_c + f_m)t + \theta_m + \phi_m(t)] \quad (7)$$

where B_m is a constant amplitude, f_m is the difference in the frequency allocation of the two carriers and θ_m denotes the lack of coherence between $s(t)$ and $i_m(t)$ and is assumed to be uniformly distributed over $(0,2\pi]$. Furthermore, $\phi_m(t)$ is given by

$$\phi_m(t) = \pi\sum_i c_i\int_{-\infty}^{t} g(\gamma - iT - \tau_m)d\gamma \quad (8)$$

where c_i are independent and equiprobable bits taking values from the alphabet $\{\pm 1\}$ and τ_m is the timing offset between $s(t)$ and $i_m(t)$. τ_m is assumed to be uniformly distributed over the time interval $(0,T]$.

In general, there are two adjacent channel interferers which contribute most significantly to the degradation of telecommunication systems. Both of them are located adjacent in the frequency domain to the channel through which the information signal is transmitted. We will therefore adopt the ACI model which is illustrated in a block diagram form in Fig. 5a. Assuming that both interferers are symmetrically located in the frequency domain around f_c, the carrier frequency of the upper interferer, which will be denoted as $i^+(t)$, is $f_c + f_m$, whereas the carrier frequency of the lower interferer, denoted as $i^-(t)$, is $f_c - f_m$. In addition to the static ACI environment, we will consider the case where all three signals under consideration could be also faded by three independent but statistical identical fading signals $f^i(t)$ with $i \in \{\pm, 0\}$. The complete channel model considered in this paper is illustrated in Fig. 5a, where the two switch positions indicate that we have either a static channel (SC) or a faded channel (FC). The fading signals $f^i(t)$ are generated as discussed in [17] and have Rayleigh statistical characteristics employing the land-mobile fading model with a normalized to T Doppler shift of F_DT [18]. After the addition of the white Gaussian noise $n(t)$, which has a double-sided power spectral density of $N_0/2$, the received signal $r(t)$ can be expressed as

$$r(t) = s''(t) + i^+(t) + i^-(t) + n(t) \quad (9)$$

for the static channel, and

$$r(t) = s''_f(t) + i^+_f(t) + i^-_f(t) + n(t) \quad (10)$$

for the Rayleigh fading channel. Clearly, for a linear channel, i.e. without any use of the NI-QM and NLA, $s''(t) = s(t)$ or $s''_f(t) = s_f(t)$.

We conclude our discussion on the communication system model by mentioning that the receivers investigated in this work consist of a predetection 4th order Butterworth low pass filter (LPF), $H_R(f)$, with a 3-dB double-sided bandwidth B_R, followed by 1- and 2-bit differential detectors without and with feedback. As previously mentioned, we will be refering to these receivers as "conventional differential detectors" (C-DD) and "decision feedback differential detectors" (DD-DF), respectively. Their detailed structure has been previously presented in [4], [7].

III. Performance Evaluation Results and Discussion

The communication system which was described in the previous section was extensively evaluated by means of computer simulation using Monte-Carlo error counting techniques. For all three GMSK transmitters, we have assumed that $B_tT = 0.3$ as this is the specification adopted by the pan-European digital cellular network [2]. The B_RT product of the predetection filter $H_R(f)$, was choosen to be equal to 0.97 for all the receivers (with or without feedback) employing 1-bit differential detectors and 0.85 for all the receivers employing 2-bit differential detection. The reason for these choices was the near optimal performance of the receivers for these values at a bit error rate (BER) of 10^{-3} in an AGWN channel [7]. In Fig. 5b, the experimental spectrum of the received signal in a static ACI and AWGN channel is illustrated. Details of the experimental prototype set-up, which has been employed to generate this signal can be found in [21]. It should be mentioned that this hardware prototype experimental set-up has been also used to verify some of the computer simulated results reported in this paper [21].

For ACI dominated applications, normally the most important parameter influencing the BER performance is the overall adjacent channel interference power, which greatly depends upon the adjacent channel frequency spacing and the actual power of the interfering signals. For convenience we will assume that the interferers have the same transmitted power, i.e. $A_0 = B_1 = B_{-1}$. In general, the carrier-to-interference ratio (C/I_A) is defined as the ratio between the average power of the desired information signal (P_{DIS}) and the average power of the adjacent interfering signals (P_{AIS}), both measured at the output of $H_R(f)$, i.e.

$$\frac{C}{I_A}\Big|_{dB} = 10\log_{10}\frac{P_{DIS}}{P_{AIS}}. \qquad (11)$$

For a given B_tT and B_RT, C/I_A will be controlled by changing the adjacent channel spacing frequency f_m, or equivalently the normalized to the rate of transmission adjacent channel spacing frequency $F_m = f_mT$. Clearly, the smaller F_m becomes, i.e. the more closer the adjacent channel interferer are to the main channel, the larger C/I_A becomes. However, at the same time, the overall spectral efficiency is increasing. Similar to [19], here we define the spectral efficiency η as the inverse of F_m, i.e. $\eta = 1/F_m$.

In the next two subsections, we will be presenting BER performance evaluation results for the linear and the nonlinear channel.

A. Linear Channel

As illustrated in Fig. 5a, for the linear channel $s''(t) = s(t)$, i.e. the NI-QM and NLA are not present. By means of computer simulation, we have first numerically computed the amount of C/I_A which is introduced as a function of F_m for both 1-bit and 2-bit DF-DD receivers. The obtained results are illustrated in Fig. 6, where we note that the results are different for the two types of receivers. This is solely due to the fact that the B_RT of the two types of receivers is different and clearly does not depend on the operating signal-to-noise ration (SNR) and fading. The performance of 1- and 2-bit C-DD and DF-DD receivers was evaluated in both static (i.e. nonfaded) and Rayleigh faded ACI and AWGN channels. Fig. 7 illustrates the BER performance evaluation results for the static ACI at $C/I_A = 15$ dB where it is clear that the DF-DD receivers outperform the C-DD receivers. For example, at a BER $= 10^{-3}$, the 2-bit DF-DD receiver results in performance gains of more than 6 dB as compared to the equivalent 2-bit C-DD receiver. Clearly these significant performance improvements are due to the fact that the DF-DD technique results in an increased opening of the eye-diagram which improves the detection. This increased eye opening is illustrated in Fig. 8 for the 2-bit C-DD and DF-DD receivers at a $C/I_A = 15$ dB. We also note that the gains for the 1-bit DF-DD receiver as compared to the 1-bit C-DD receiver are even higher. Additional BER performance evaluation results, which have been presented in [21], have indicated that by increasing the C/I_A, the performance gains are increasing, whereas by decreasing C/I_A, these gains are also decreasing.

Further performance evaluation results, which due to space limitations will not be presented here, can be found in [21].

B. Non-Linear Channel

For the nonlinear channel, we assume that, as illustrated in Fig. 5, the NI-QM and the NLA are present. Since the nonlinearities cause spectral spreading, new C/I_A versus F_m curves need to be computed first. It has been shown in [21], that the C/I_A curves for the nonideal GMSK system with typical values of QM errors are almost identical as those for the ideal GMSK system. However, for the extreme values of QM errors, these curves are noticable different. For example, as illustrated in Fig. 9, for the 2-bit differential receiver and for extreme values of QM errors, C/I_A

drops significantly especially when a HL is employed. This is due to the spectral spreading caused by the nature of the extreme nonlinear function of the HL [16]. Similar results have been obtained for the 1-bit differential receiver [21].

Figs. 10 and 11 illustrate typical BER performances of the various differential receivers under investigation for a stactic ACI with $C/I_A = 15$ dB and 20 dB, respectively. For all systems, it has been assumed that a NI-QM with extreme values of QM errors and a HL are employed. From both figures it is clear that the DF-DD receivers perform much better than the C-DD receivers, with the 1-bit DF-DD receiver outperforming the other receivers.

Further performance evaluation results, which due to space limitations will not be presented here, can be found in [21].

REFERENCES

[1] K. Murota and K. Hirade, "GMSK modulation for digital mobile radio telephony," *IEEE Trans. Commun.*, vol. COM-29, pp. 1044-1050, July 1981.

[2] D. J. Goodman, "Second generation of wireless information networks," *IEEE Trans. Veh. Techn.*, vol. VT-40, pp. 366-371, May 1991.

[3] ETSI, Digital European Cordless Telecommunications - Common Interface, Radio Equipment and Systems, Valborne, France, 1990.

[4] A. Yongacoglu, D. Makrakis and K. Feher, "Differential detection of GMSK using decision feedback," *IEEE Trans. Commun.*, vol. COM-36, pp. 641-648, June 1988.

[5] F. Adachi and K. Ohno, "Performance analysis of GMSK frequency detection with decision feedback equalisation in digital land mobile radio," *IEE Proceedings, Part F*, vol. 135, pp. 199-207, June 1988.

[6] I. Korn, "GMSK with differential phase detection in the satellite mobile channel," *IEEE Trans. Commun.*, vol. COM-38, pp. 1980-1986, Nov. 1990.

[7] S. S. Shin and P. T. Mathiopoulos, "Differentially detected GMSK signals in CCI channels for mobile cellular telecommunication systems," *IEEE Trans. Veh. Techn.*, vol. VT-42, pp. 289-293, Aug. 1993.

[8] W. C.-Y. Lee, *Mobile Cellular Telecommunications.* 2nd Edition, McGraw-Hill, 1995.

[9] L. B. Milstein, R. L. Pickholtz and D. L. Schilling, "Comparison of performance of digital modulation techniques in the presence of adjacent channel interference," *IEEE Trans. Commun.*, vol. COM-30, pp. 1984-1993, Aug. 1982.

[10] S. Golestaneh, H. M. Hafez and S. A. Mahmoud, "The effects of adjacent channel interference on the capacity of FDMA cellular systems," *IEEE Trans. Veh. Techn.*, vol. VT-43, pp. 946-954, Nov. 1994.

[11] K. Feher, *Advanced Digital Communications.* Prentice Hall, 1987.

[12] G. C. Hess, *Land-Mobile Radio System Engineering.* Aertech House, 1993.

[13] I. Korn, "Differential phase shift keying in two-path Rayleigh channel with adjacent channel interference," *IEEE Trans. Veh. Techn.*, vol. VT-40, pp. 461-471, May 1991.

[14] S. Ariyavisitakul and T. Liu, "Characterizing the effects of nonlinear amplifiers on linear modulation for portable radio," *IEEE Trans. Veh. Techn.*, vol. VT-39, pp. 383-389, Nov. 1990.

[15] C.-E. Sundberg, "Continuous phase modulation," *IEEE Comm. Mag.*, vol. 24, pp. 25-38, Apr. 1986.

[16] A. E. Jones, T. H. Wilkinson, and J. G. Gardiner, "Effects of modulator deficiencies and amplifier nonlinearities on the phase accuracy of GMSK signalling," *IEE Proceedings, Part I*, vol. 140, pp. 157-163, Apr. 1993.

[17] D. Makrakis, P. T. Mathiopoulos and D. P. Bouras, "Optimal decoding of coded PSK and QAM signals in correlated fast fading channels and AWGN: A combined envelope, multiple differential and coherent detection approach," *IEEE Trans. Commun.*, vol. COM-42, pp. 63-77, Jan. 1994.

[18] L. J. Mason, "Error probability evaluation for systems employing differential detection in a Rician fast fading environment and Gaussian noise," *IEEE Trans. Commun.*, vol. COM-35, pp. 39-46, Jan. 1987.

[19] T. Le-Ngoc and K. Feher, "Performance of IJF-OQPSK modulation schemes in a complex interference environment," *IEEE Trans. Commun.*, vol. COM-31, pp. 137-144, Jan. 1983.

[20] M. Faulkner and T. Mattson, "Spectral sensitivity of power amplifiers to quadrature modulator misalignment," *IEEE Trans. Veh. Techn.*, vol. VT-41, pp. 516-525, Nov. 1992.

[21] J. S. Toor, *Differentially Detected GMSK Systems in the Presence of Adjacent Channel Interference and Nonlinearities*, M.A.Sc. Thesis, Department of Electrical Engineering, The University of British Columbia, July 1994.

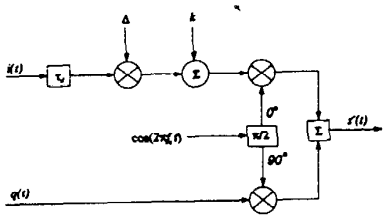

Fig. 1

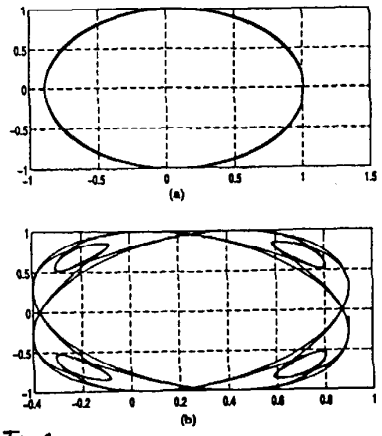

Fig. 2

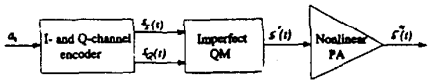

Fig. 3

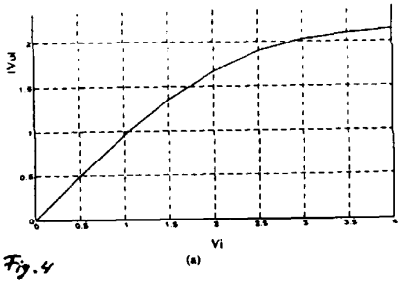

Fig. 4

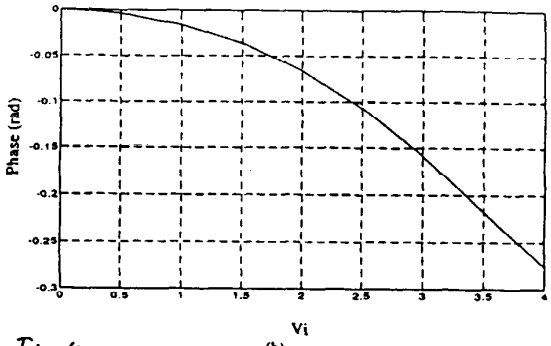

Fig. 4

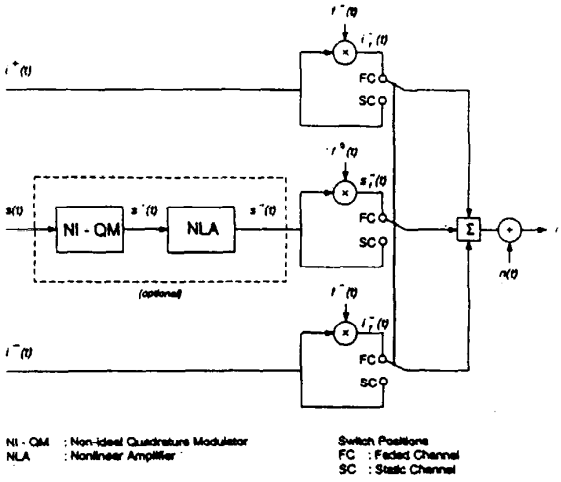

Fig. 5(a)

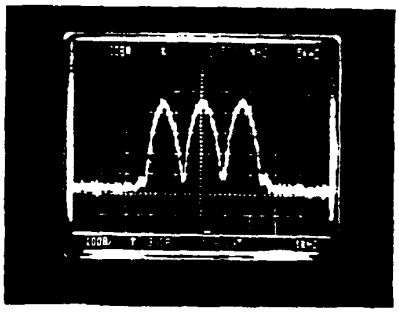

Fig. 5(b)

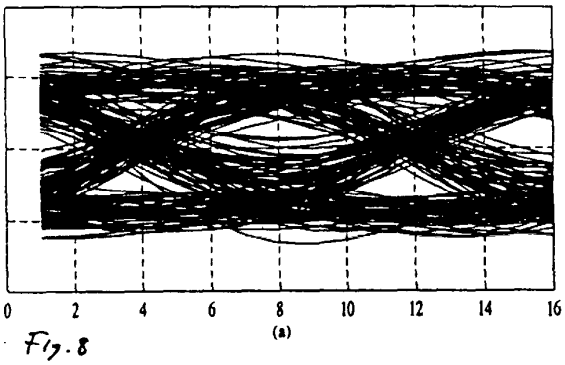

Fig. 8

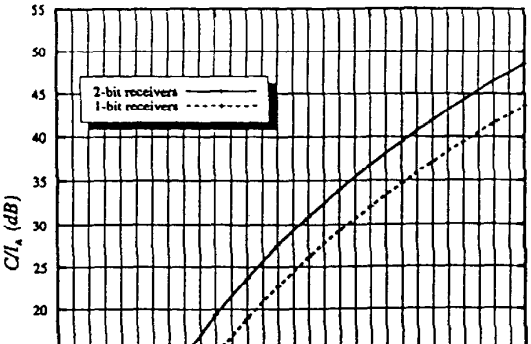

Fig. 6

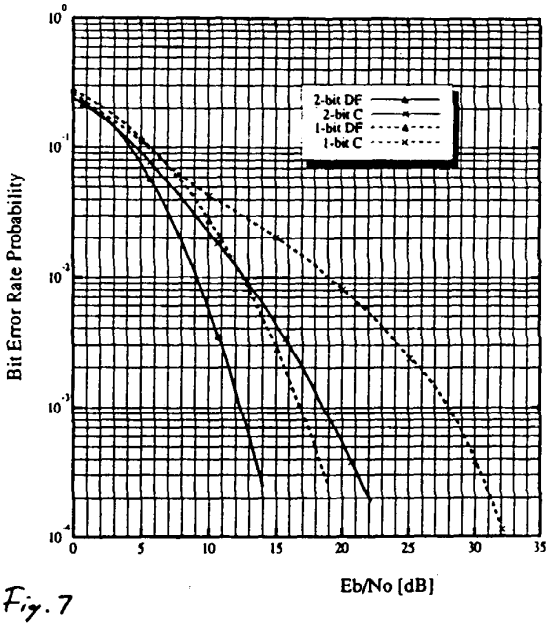

Fig. 7

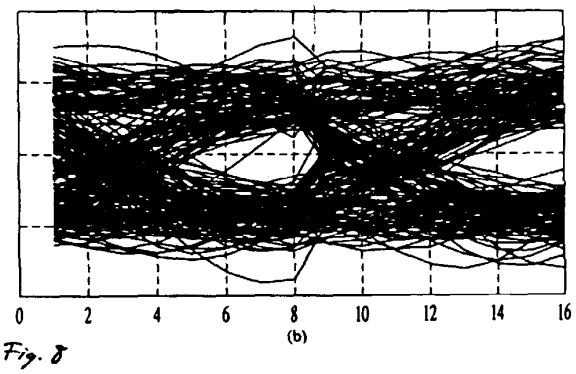

Fig. 8

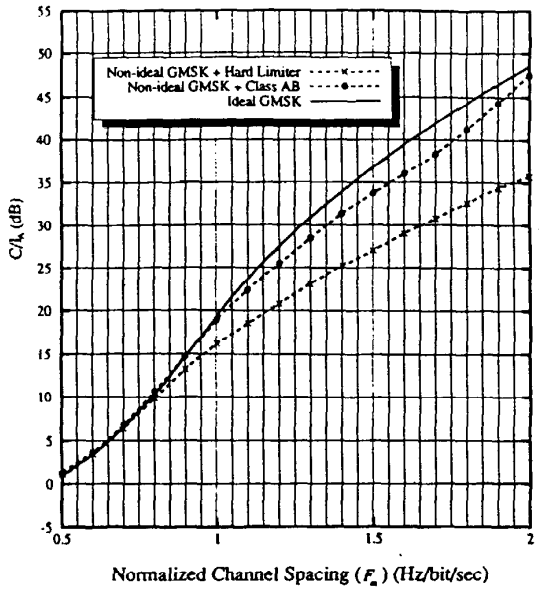

Fig. 9

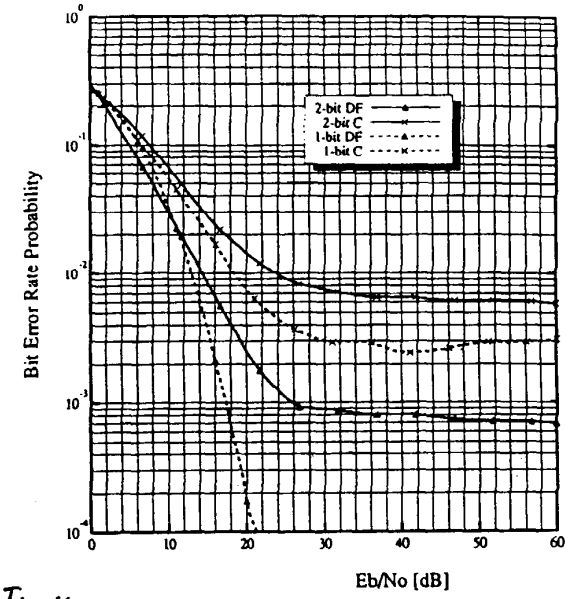

Fig. 11

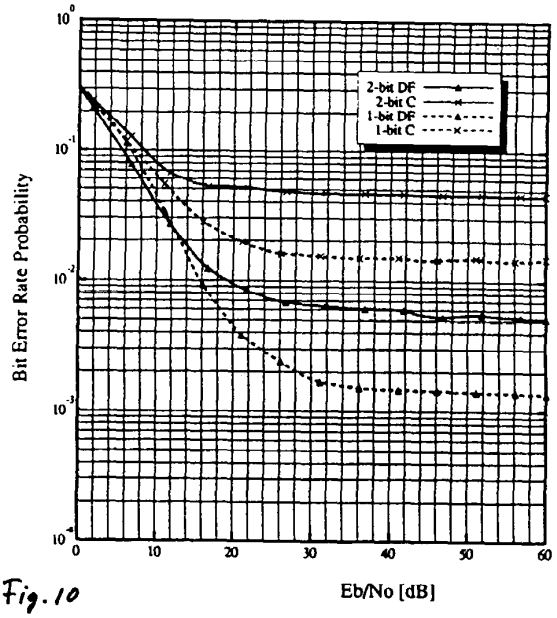

Fig. 10

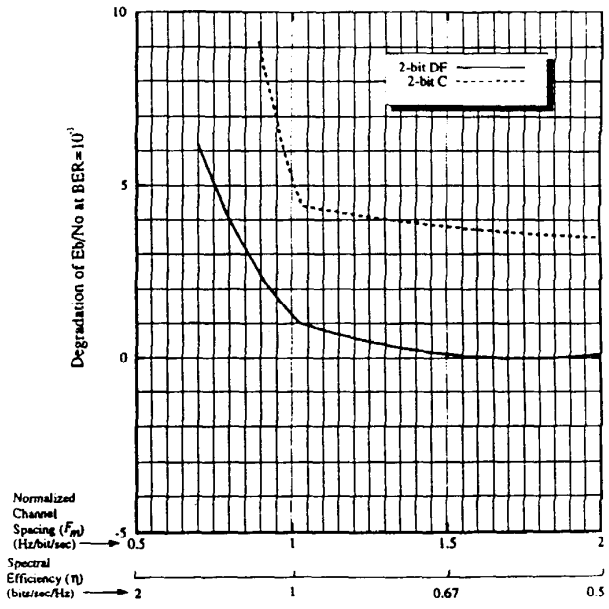

Fig. 12